Geoderma 221–222 (2014) 70–81

Contents lists available at ScienceDirect

Geoderma

journal homepage: www.elsevier.com/locate/geoderma

# The role of mineral soil topography on the spatial distribution of organic layer thickness in a paludified boreal landscape

Ahmed Laamrani [a,*], Osvaldo Valeria [a,1], Nicole Fenton [a,2], Yves Bergeron [a,3], Li Zhen Cheng [b,4]

[a] Institut de recherche sur les forêts (IRF), Université du Québec en Abitibi-Témiscamingue (UQAT), 445 boul. de l'Université, Rouyn-Noranda, Québec J9X 5E4, Canada
[b] Institut de recherche en mines et environnement (IRME), UQAT, 445 boul. de l'Université, Rouyn-Noranda, Québec J9X 5E4, Canada

ARTICLE INFO

*Article history:*
Received 10 July 2013
Received in revised form 2 December 2013
Accepted 2 January 2014
Available online 28 January 2014

*Keywords:*
Paludification
Soil organic layer depth
Boreal forest soil
Mineral soil topography
Regression tree
LIDAR-derived DTM

ABSTRACT

Mineral soil topography is difficult to describe in boreal regions because of the thick overlying organic layer despite its presumed importance in determining where and at what rate an organic layer will accumulate (paludification). The overall purpose of this study was to examine the relationship between mineral soil topography and OLT at the landscape scale. More specifically, these relationships can be used to map the distribution and spatial variability of paludification across the landscape, thereby exploring the potential to discriminate between the two commonly known paludification types (permanent and reversible). Seven topographic variables (elevation, slope, aspect, mean curvature, plan curvature, profile curvature and topographic wetness index) were generated from a digital elevation model that we developed for the mineral soil surface (MS-DEM). OLT data were collected from field measurements across the landscape by manual probing and values varied from 5 to 150 cm. The MS-DEM was generated by subtracting OLT field values from the corresponding LiDAR-derived elevation values. Most correlations between OLT and individual predictor variables were weak and illustrated that OLT and its landscape-scale distribution cannot be explained by simple bivariate relationships. Consequently, two regression tree-based models were developed using: (1) only the seven mineral soil topographic variables, and (2) all predictor variables (mineral soil topography and surficial deposits). Mineral soil slope was the most important variable for both models and corresponded to the first level of splitting the dataset into homogenous landscape units in terms of organic layer thickness. Surficial deposit, topographic wetness index (TWI) and aspect were also related to OLT and proved to be contributing to the development of the two models.
Model 1 explained 0.34 of the OLT variability and offer simple models with few landscape units that are easy to interpret. Model 1 splitting rules allowed the combination of different maps (slope, TWI and aspect) for producing a landscape units map, on which OLT was determined and related to increasing paludification categories. A good overall accuracy of 74% was achieved for this map. Model 2 was the best model in terms of estimate quality ($R^2_{adj} = 0.52$). Both models were successful in discriminating highly paludified landscape units. Except for one landscape unit that was assigned to permanent paludification type, both models were unable to further subdivide more landscape units into reversible and permanent paludification, suggesting that both of these types interact within the same landscape unit. This study demonstrated that the combination of topographic information from remotely sensed LiDAR data and field OLT measurement data has the potential to be useful for defining both promising and vulnerable areas for forest management.



## 1. Introduction

Paludification is a natural process where organic material accumulates on the ground surface over time, resulting in higher soil moisture levels and elevated water tables (Crawford et al., 2003; Vygodskaya et al., 2007). These conditions alter dynamic succession and favour the invasion of *Sphagnum* moss species (Fenton and Bergeron, 2006, 2007; Fenton et al., 2005), which can lead to the development of forested peatlands and substantial decreases in forest productivity (Simard et al., 2007, 2009). While essentially a regional process, many parts of the world, including interior Alaska, the western Siberian plain, and the Hudson Bay–James Bay Lowlands of Canada, are prone to paludification. In the black spruce forests of the Clay Belt, a region in the southern portion of the Hudson Bay–James Bay Lowlands (Fig. 1A), time-since-last fire and ground surface topography have been reported as the two main factors that cause paludification. Consequently, two types of paludification can be identified: permanent and reversible, respectively (Fenton et al., 2009; Lavoie et al., 2007; Simard

* Corresponding author. Tel.: +1 819 732 8809x8240.
*E-mail addresses:* Ahmed.Laamrani@uqat.ca (A. Laamrani), Osvaldo.Valeria@uqat.ca (O. Valeria), Nicole.Fenton@uqat.ca (N. Fenton), Yves.Bergeron@uqat.ca (Y. Bergeron), Li_Zhen.Cheng@uqat.ca (L.Z. Cheng).
[1] Tel.: +1 819 762 0971x2384.
[2] Tel.: +1 819 762 0971x2312.
[3] Tel.: +1 819 762 0971x2347.
[4] Tel.: +1 819 762 0971x2351.

0016-7061/$ – see front matter © 2014 Elsevier B.V. All rights reserved.
http://dx.doi.org/10.1016/j.geoderma.2014.01.003

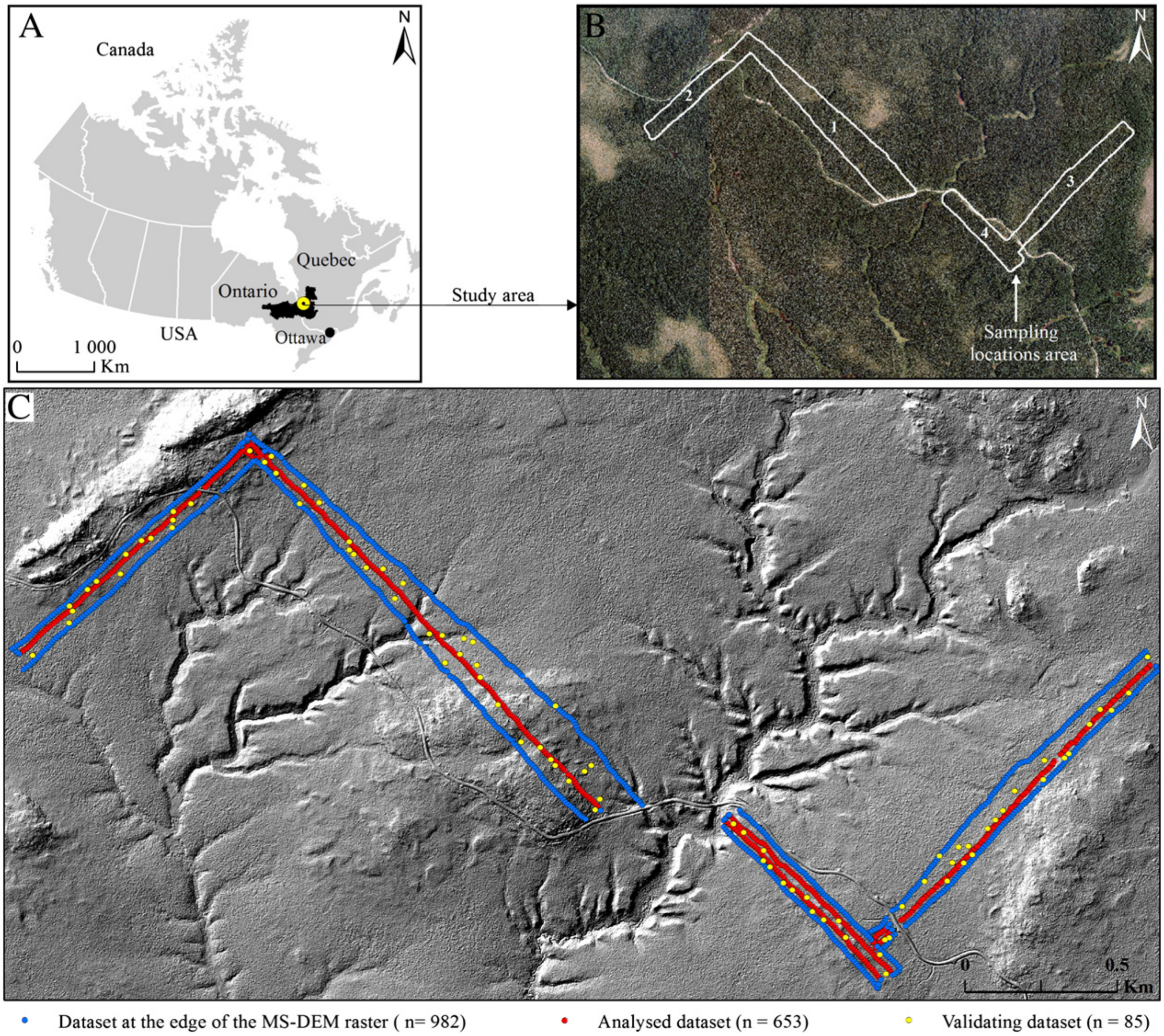


**Fig. 1.** Study area within the Clay Belt of Ontario and Quebec (A). Sampling locations along transects within four sectors (1, 2, 3, and 4) and delimitation of the mineral soil digital elevation model area (B). Landscape map of the study area showing the field organic layer thickness sampling points locations (C). The analysed dataset ($n = 653$) was formed by summing the original dataset along the central transects ($n = 568$) and independent validation datasets along the same transects ($n = 85$).

et al., 2007). Within the landscape, permanent paludification dominates in natural depressions, which have wetter soil conditions that favour organic layer build-up. Reversible paludification occurs on flat or sloping terrain, where a feather moss-dominated bryophyte layer is replaced over time by Sphagnum species, starting about 100 years following fire (Fenton and Bergeron, 2006; Simard et al., 2007).

Numerous studies have been conducted to characterise the influence of topography on the accumulation and spatial variability of the organic layer across the Clay Belt (i.e., Giroux et al., 2001; Lavoie et al., 2005, 2007; Simard et al., 2009); however, these studies have largely been restricted to investigations of the ground surface topography at the plot-scale. In a recent extensive study at the landscape scale, Laamrani et al. (2013b) found weak correlations between organic layer thickness (OLT) and topographic surface variables, suggesting that OLT may be controlled by other factors, such as the mineral soil topography, i.e., the contours of the surface beneath the organic layer.

Mineral soil topography affects the accumulation of organic layer mainly through its control of water movement at the landscape scale (Emili et al., 2006). This topography has been difficult to describe in boreal regions because it is masked by the thick overlying organic material. Despite the presumed importance of mineral soil topography in determining where and to what degree paludification will occur in the Clay Belt, no attempt has been made in this region until now to measure and link mineral soil topography to OLT and to the two paludification types (permanent and reversible) at the landscape scale. In this context, the overall purpose of this study was to examine the relationship between mineral soil topography and OLT at the landscape scale. More specifically, these relationships can be used to map the distribution and spatial variability of paludification across the landscape, thereby exploring the potential to discriminate between permanent and reversible paludification. To do so, we correlated field organic layer measurements that were obtained by manual probing with topographic variables that were derived from a digital elevation model (DEM), which was generated at the mineral soil surface. The mineral soil DEM was generated using LiDAR (Light Detection And Ranging) data together with field OLT measurements.

## 2. Methods and materials

### 2.1. Study area

The study was located in the James Bay Lowlands physiographic region of Quebec, Canada (Fig. 1A). It was centred (49°27′30″ N, 78°31′5″ W) on a 72 ha site within the Clay Belt region, which is dominated by black spruce (*Picea mariana* [Mill.] BSP) forest (Fig. 1B). The forest floor was composed of *Sphagnum* spp., feather mosses (principally

*Pleurozium schreberi* (Brid.) Mitten), and shrubs, (mainly dwarf ericaceous species), with variable coverage across the landscape. This region has low topographic relief, as the Canadian Shield was overlain by extensive clay deposits by pro-glacial Lakes Barlow–Ojibway (Veillette, 1994). Within the study area, ground surface slope ranged from 0.3 to 15.7%; about 60% of the area has a slope greater than 2%. Elevation ranged from 290 m to 314 m above sea level (mean = 303 m).

OLT varied from 5 to 150 cm across the landscape. The underlying mineral soil is variable, ranging in composition from clay to till. The thickness of the mineral layer over bedrock is variable across the landscape, ranging from 1 m (Laamrani et al., 2013a) to 60 m (Veillette et al., 2005). A detailed description of mineral deposits present in the study area has been provided in Veillette et al. (2005). The study area is underlain by bedrock, which is a complex mixture of Precambrian granitic rock types that occasionally appear at the ground surface and which form scattered gentle hills across the landscape. Many streams run locally in a southwestern direction through the area, which produced a relatively complex topographic pattern within the landscape (Fig. 1C). At the La Sarre weather station, located at about 85 km southwest of the site, mean annual temperature is 0.7 °C and total annual precipitation is 890 mm (Environment Canada, 2013).

### *2.2. Sampling design and field data collection*

The objectives of this study were addressed by establishing thirteen sub-parallel transects through forest stands within the study area (Fig. 1B). The thirteen transects, totalling 15 km in length, were established across four different sectors (1, 2, 3, and 4; Fig. 1B), which covered a variety of sites that differed in OLT, degree of paludification, drainage, vegetation cover, and substrate moisture conditions. This transect configuration took a long time to complete but provided an extra dimension that was important for interpreting the mineral soil topography. This also permitted us to generate a spatially continuous cross-sectional profile of the mineral soil topography. A minimum distance of 20 m was maintained between transects in order to optimise lateral interpolation between transects.

Field organic layer measurements (response variable) were collected at 10 m intervals along each transect by probing with a manual auger ($n = 1550$). At each sampling point, the auger bored through the organic layer until the mineral soil was encountered. The auger was then removed and the marked depth to mineral soil was accurately measured. The thickness of the organic material was taken as the distance between the organic layer surface and the mineral soil interface. In nearly all cases, the transition between organic layer and mineral soil was clearly marked by an obvious change in colour and texture. An additional 172 OLT measurements were also collected over the study area and used for validation purposes (Fig. 1C). These 172 sampling points were randomly disturbed between transects ($n = 85$) and along the central transect ($n = 87$). Each organic layer measurement along the central transect was located halfway between two sampling points established at 10 m intervals. Two locations along the central transects had to be excluded, as it was technically impossible to measure OLT because they were located in deep depressions; consequently, the exclusion of two sites, which should not affect the results, reduced the validation dataset to 170 sampling points.

At every sampling point, the presence of each organic horizon and the nature of the underlying mineral material (clay, till, bedrock) were recorded in the field. The spatial distribution, stratigraphy and origin of the surficial deposits were highly variable across the study area. It should be mentioned that surficial deposits nomenclature (clay, till, bedrock) used in this study referred to the mineral material underlying the organic layer. In the present study, "bedrock" referred to unconsolidated material (also called regolith) overlying solid rock. To correlate each type of surficial deposits (clay, till, bedrock) with organic layer thickness, surficial deposits were considered as a factor, taking nominal values of 0 for till, 1 for clay, and 2 for bedrock.

### *2.3. Mineral soil topography*

#### *2.3.1. Generation of mineral soil digital elevation model*

Prior to the creation of a mineral soil digital elevation model (MS-DEM), a digital terrain model (DTM) was generated based on LiDAR data (with ±0.065 m vertical accuracy and 15-m resolution). The latter is becoming one of the most effective and reliable remote sensing technologies for assessing topography at both the plot- and landscape-scales in boreal forested environments (i.e., Laamrani et al., 2013b; Southee et al., 2012; Webster et al., 2011; Work et al., 2011). Laamrani et al. (2013b) and Vepakomma et al. (2011) described in detail the processing and creation of the LiDAR-derived DTM.

Positions of all field sampling measurements (along transects and plots) were recorded using a Trimble GeoXT handheld GPS to provide 50 cm-level positioning accuracy and to allow direct comparison with the DTM. The field OLT dataset was then superimposed upon the DTM and surface topography elevations were extracted for each sampling location. By subtracting the OLT values from the corresponding DTM values at each field point, a new dataset of mineral soil elevations was obtained for the study area. This new dataset was first used to create a digital representation of the three-dimensional surface using (TIN) procedure (Triangulated Irregular Networks; Peucker et al., 1978). A digital elevation of the mineral soil surface model was then created by converting the TIN to a raster format with an optimal resolution of 15 m (cell size). The resulting mineral soil digital elevation model (MS-DEM) was validated with a set of field-measured points ($n = 170$; 85 sampling points along the central transects and another 85 points between transects; Fig. 1C). This raster validation dataset was not part of the original dataset ($n = 1550$) that was used to produce the MS-DEM (Fig. 1C).

#### *2.3.2. Topographic variable calculation*

Mineral soil surface topographic variables (predictor variables), which were derived from the MS-DEM, included elevation, slope, aspect, mean curvature, plan curvature, profile curvature, and a compound topographic wetness index. A detailed description of each of these topographic variables is provided in Table 1. The chosen topographic variables may aid spatial estimation of paludified areas, because the topography is presumed to have a great influence on organic layer accumulation whereby topographic lows/depressions would be associated with an accumulation of organic matter and a concomitant rise in the water table. The topographic wetness index (TWI) has been found to play a significant role in estimating different soil features that are related to paludified areas such as local soil moisture (Blyth et al., 2004; Güntner et al., 2004), horizon depth (Gessler et al., 1995; Moore et al., 1993; Seibert et al., 2007), vascular plant species richness in boreal forests (Sørensen et al., 2006; Zinko et al., 2005), and the spatial distribution of groundwater flow along forest–peatland complexes within the boreal forest (Emili et al., 2006).

Values of each of the topographic variables were calculated for each cell of the MS-DEM using ArcGIS 10 (ESRI, 2011). Conceptually, the topographic variable tool (i.e., slope, aspect) fits a plane to the z-values of a 3 × 3 cell neighbourhood around the central cell. When a cell location within this nine-cell neighbourhood with a "NoData" z-value, the z-value of the central cell was assigned to the location, after which the topographic variable was then computed. At the edge of the MS-DEM raster, at least three cells (outside the raster's extent) contained NoData as their z-values. For mineral soil slope calculation, for instance, this problem resulted in a flattening of the 3 × 3 plane fitted to these edge cells, which leads to a decrease in the slope (ESRI, 2011), and thus to a biased value of this topographic variable. To avoid including biased values from cells next to the physical edge of the MS-DEM raster, OLT measurement corresponding to cells that had at least one NoData cell as a neighbour was excluded from the analysed dataset. These excluded data were located mainly along transects at the edge of the MS-DEM raster (Fig. 1C). In addition, simple correlations between OLT and the

**Table 1**
Description of the topographic variables that were derived from the mineral soil digital elevation model (MS-DEM).

| Topographic variables | Description |
|---|---|
| Elevation | Height above sea-level of a particular mineral soil location. Mineral soil $z$-value was calculated for each sampling location as the difference between the LiDAR DTM and the organic layer thickness at that location. |
| Slope | Calculated for each grid cell as the maximum rate of change in $z$-value from that cell to its neighbours. Slope affects the overall rate of movement downslope. |
| Aspect | Direction of the maximum rate of change in the z-value from each cell to its neighbours. Aspect defines the direction of flow and was classified into four major classes, viz., North, East, South and West. |
| Mean curvature | A general measure of the convexity of the landscape, where sinks and valleys are considered concave (negative values), and peaks and highs are considered convex (positive values). |
| Plan curvature | Curvature of the surface perpendicular to the slope direction. (+) values indicate that water flow would diverge (convex surface), whereas (−) values indicate that water flow would converge (concave surface). |
| Profile curvature | Curvature of the surface in the direction of slope. (+) values indicate that water flow would decelerate (concave surface), whereas a (−) values will indicate that water flow would accelerate (convex surface). |
| Topographic wetness index | $TWI = \ln(A_s/\tan\beta)$ (Moore et al., 1993). $A_s$ is the local upslope contributing area and $\beta$ is the local slope. The higher the value of the TWI in a cell, the higher the soil moisture and water accumulation that can be found on it. |

topographic variables showed that when data from cells next to the physical edge of the MS-DEM raster were excluded, relationships were improved for most topographic variables. For instance, TWI, slope and elevation correlations were improved by 17%, 9% and 4%, respectively; this rationalises our use of a reduced dataset ($n = 653$) for subsequent analyses, rather than the entire dataset, which was used to generate the MS-DEM ($n = 1550$). The reduced dataset is referred to in this study as the "analysed dataset" and consisted of the sum of central transect sampling points ($n = 568$) and the validation dataset sampling points along the central transect ($n = 85$), for a total of 653 sampling points.

### 2.4. Relating topography variables and OLT

To investigate relationships between predictor variables (topographic variables and surficial deposits) and the response variable (field-measured organic layer thickness), we used Spearman's rank correlation and regression tree modelling, which are both non-parametric methods. Spearman rank correlation ($r_s$) was used instead of the usual parametric Pearson product–moment correlation. In the latter variables are presumed to have a linear relationship, which was not the case of the entire dataset used in this study. For these reasons, no attempt was made to explore the relationships between predictor and response variables using linear mixed-effects models.

Regression trees are well-suited to the analysis of our datasets because of their (i) capability in modelling both complex and non-linear relationships (Greve et al., 2012a; Rothwell et al., 2008) between covariates and response variables, which can be easily interpreted and discussed (Bou Kheir et al., 2010); (ii) ability of handling both categorical (i.e., surficial deposits) and quantitative (i.e., elevation and slope) data (Greve et al., 2012b; Johnson et al., 2009); further, (iii) recursive partitioning of the dataset into more homogeneous groups allows the identification of potential relationships between the response variable (in our case, organic layer thickness) and the environmental predictors, while also identifying interactions among these latter independent variables (Rothwell et al., 2008).

In the present study, regression trees were used to split the landscape OLT data into different homogeneous spatial units (also known as terminal nodes). In this study, the terminal nodes were named as "landscape units" that refer to relatively homogeneous areas in term of OLT distribution. Splits or rules defining how the data were to be partitioned were selected based on a significance test of independence between covariates and the response variable. A split was established when the $P$-value was smaller than $\alpha = 0.05$. In other words, the split was established when the global null hypothesis of independence between the response variable and any of the predictors could not be rejected at $\alpha = 0.05$ (Hothorn et al., 2006). Unlike other decision tree methods (e.g., CARTs), there was no need for the regression tree modelling approach used in this study for using post hoc pruning to prevent overfitting since $P$-values were used as the stopping criterion (Everitt and Hothorn, 2009).

In this study, individual predictor variables that were significantly correlated with organic layer (Table 2) and surficial deposits were used to develop two regression tree-based models. Model 1 was developed using only the mineral soil topographic variables (slope, aspect, mean curvature, plan curvature, profile curvature, and TWI) that had been directly derived from the MS-DEM. Model 2 was developed using all of the predictor variables (mineral soil topography and surficial deposits). Once the regression trees were completed, they provided a set of decision rules that defined the range of conditions, i.e., values of the predictor variables, which are best used to predict each landscape unit. Predictive maps of OLT could then be created through the application of the subsequent splitting rules using ArcGIS 10.0 (ESRI, 2011). Mean values of OLT in the resulting landscape units were then used to classify them into one of four categories of increasing paludification: null (0–25 cm); low (26–40 cm); moderate (41–60 cm); and high (>60 cm). This classification scheme was inspired by previous studies from the same region (Beaudoin et al. unpublished results; Laamrani et al., 2013b; Simard et al., 2009). The resulting predictive paludification categories were verified against OLT field measurements ($n = 85$) using datasets that were randomly selected between the transects sampling locations (Fig. 1C) and were not used in regression tree development. The validation procedure, of the resulting map and paludification categories, was based on conventional confusion matrix procedure, using overall accuracy and producer accuracy following Congalton (1991).

Assumptions regarding the lack of multicollinearity (Variance inflation factors), normality of the data (Shapiro–Wilk test), and equal error variance (homoscedasticity, Levene's test) of the regression models were satisfied. Significance was declared at a level of $\alpha = 0.05$, with all statistical analyses were performed in R (R Development Core Team, 2011). Regression trees were realised using the *ctree* function in the *party* package (Hothorn et al., 2006).

## 3. Results

### 3.1. Importance of individual predictor variables

Analyses revealed that among all of the mineral soil surface topographic variables, the highest correlations with OLT were exhibited by slope ($r_s = -0.54$, $P < 0.001$) and TWI ($r_s = 0.40$, $P < 0.001$). When the data were stratified according to aspect, these coefficients were even higher, especially for south-facing areas (Slope, $r_s = -0.66$, $P < 0.001$; TWI, $r_s = 0.56$, $P < 0.001$; Table 2 and Fig. 2). Elevation had a weak relationship with OLT measurements ($r_s = 0.15$, $P < 0.001$), and shallow and thick organic layers occurred at both high and low elevations in the study area (Fig. 2). When stratified by aspect, the correlation between elevation and OLT was only significant for west-facing sites ($r_s = 0.36$, $P < 0.001$). The positive relationship between elevation and OLT could be attributable to thick organic layers accumulating over mineral soil on plateaus (flat areas at higher elevation). Because of this

**Table 2**
Relationships between organic layer thickness and topographic variables, where the latter values were extracted from the mineral soil digital elevation model (MS-DEM).

| Topographic variables | All data[a] | | | | | $r_s$[b] | | | | $r_s$[c] | | |
|---|---|---|---|---|---|---|---|---|---|---|---|---|
| | Min | Mean | Max | SD | $r_s$ | North | East | South | West | Till | Clay | Bedrock |
| Elevation | 290 | 303 | 314 | 5 | 0.15** | 0.04 | 0.04 | 0.06 | 0.36** | 0.22* | −0.07** | −0.33* |
| Slope | 0.2 | 2.9 | 14.7 | 1.9 | −0.54** | −0.20 | −0.27† | −0.66** | −0.44** | −0.15* | −0.34** | 0.03 |
| Mean curvature | −1.7 | 0.02 | 2.4 | 0.4 | 0.01 | 0.01 | 0.08 | 0.06 | −0.07 | −0.10 | 0.03 | −0.10 |
| Plan curvature | −0.7 | 0.01 | 1.4 | 0.2 | 0.02 | −0.05 | 0.01 | 0.03 | 0.02 | −0.07 | 0.04 | −0.07 |
| Profile curvature | −1 | −0.01 | 1.6 | 0.2 | −0.03 | 0.00 | −0.13 | −0.08 | 0.08 | −0.11 | −0.03 | 0.08 |
| TWI | 6 | 8 | 11 | 1 | 0.40** | 0.23 | 0.34* | 0.56** | 0.11 | 0.26** | 0.13† | 0.38* |

**, * and † statistically significant at $P < 0.001$, $<0.01$ and $< 0.05$, respectively. $r_s$ refers to Spearman's rank correlation coefficient.
[a] Analysed dataset: $n = 653$.
[b] Dataset stratified by aspect with $n_{[North]} = 51$; $n_{[East]} = 64$; $n_{[South]} = 281$; and $n_{[West]} = 257$.
[c] Dataset stratified by surficial deposit types with $n_{[Till]} = 236$; $n_{[Clay]} = 363$; and $n_{[Bedrock]} = 54$.

local pattern and the narrow range of elevations (290–314 m) over the study area, we chose to exclude elevation from subsequent analyses.

All curvature variables (mean, plan and profile) were not correlated to field measurements of OLT (Table 1), however these correlations were significant when we split each of the surface curvature topographic variables into two classes, viz., concave and convex (Fig. 3). Although the correlations were not strong ($r_s \leq 0.26$), overall OLT tended to increase with concavity.

Mean OLT overlaying the three types of surficial deposits differed significantly (Post hoc Tukey's HSD, $P < 0.0001$: clay-till, clay-bedrock and till-bedrock). Surficial deposits were significantly correlated with OLT ($r_s = 0.58$, $P < 0.001$, $n = 653$). Correlations between OLT and topographic variables were also calculated for each of the surficial deposits (clay, till, bedrock) to determine whether or not they improved with stratification by surficial deposits. Most coefficients were smaller than or not significant compared to the coefficients that had been

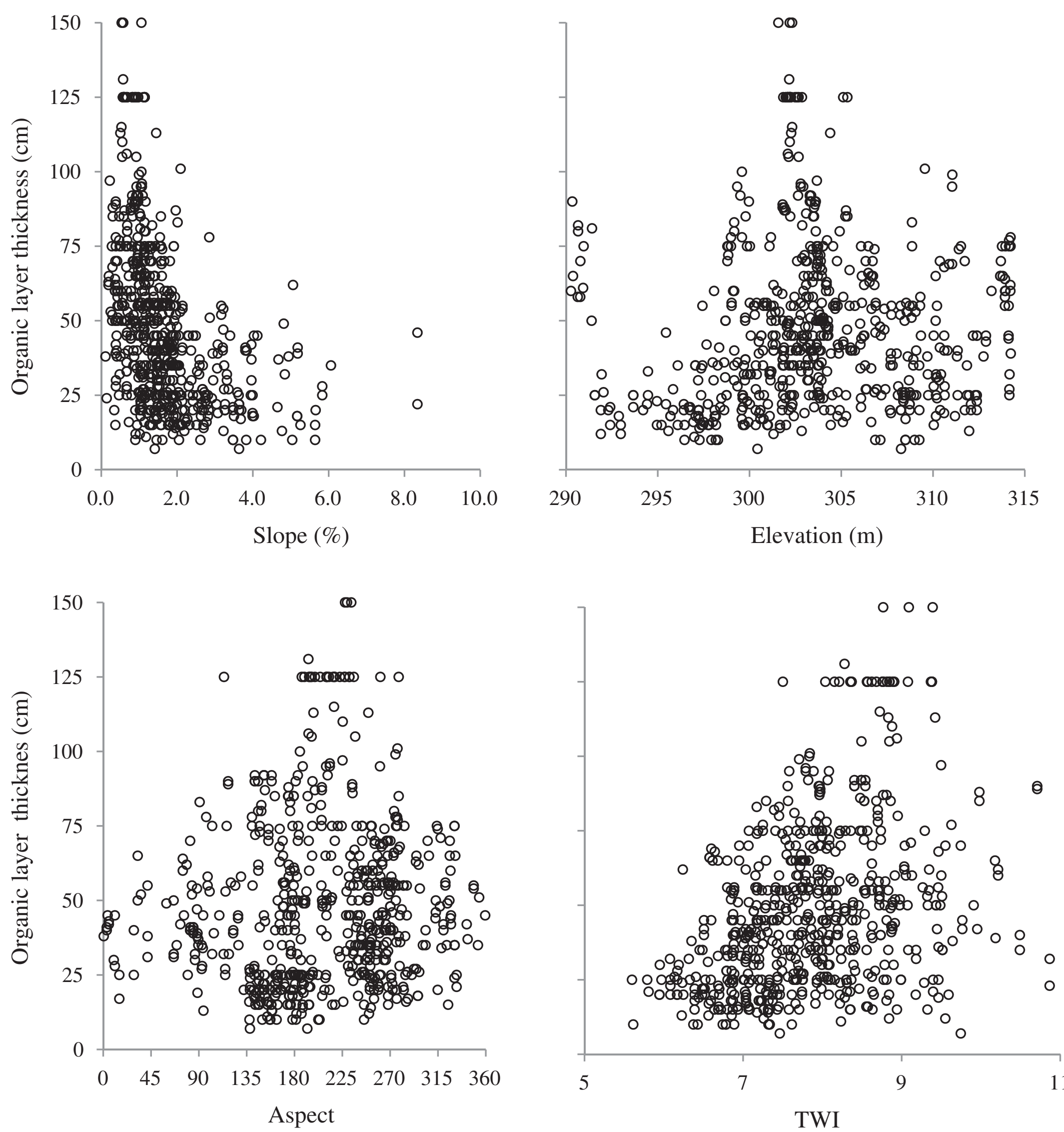


**Fig. 2.** Field measured organic layer thickness versus mineral soil surface topographic variables.

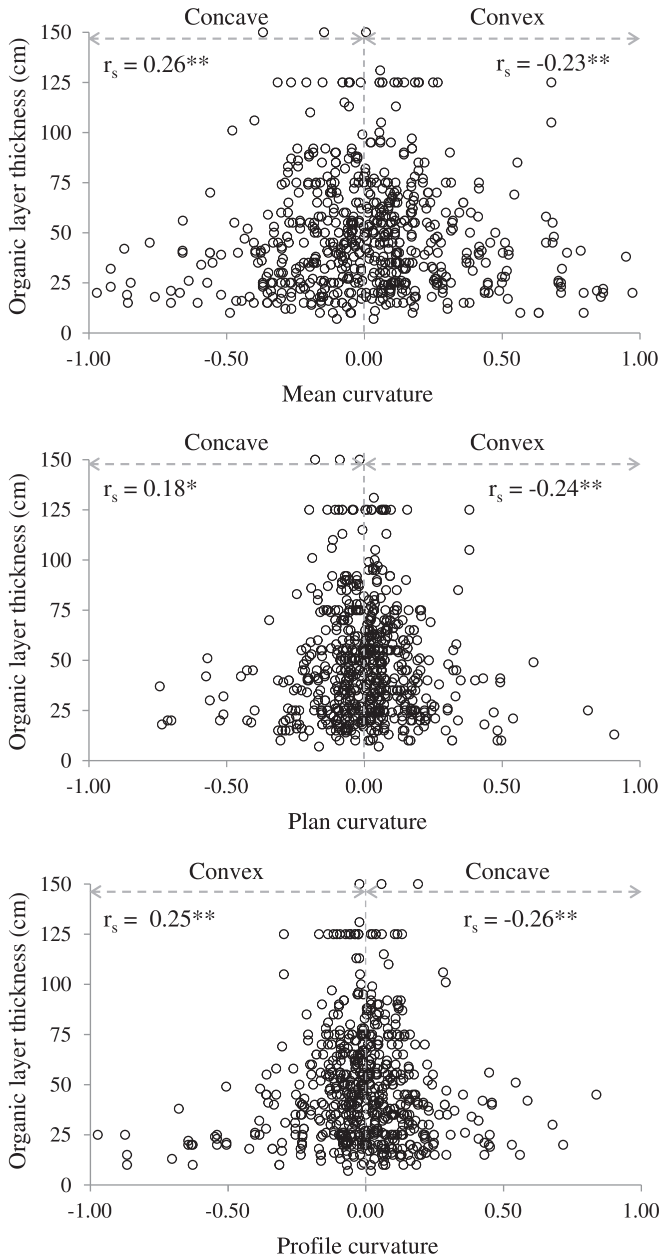


**Fig. 3.** Relationship between organic layer thickness and mineral soil curvature variables (mean, plan and profile).

calculated for the entire dataset. Of all the topographic variables that were examined, only TWI was significantly correlated with the three types of surficial deposits (Table 2). Correlations were weak but significant between OLT and clay- ($r_s = -0.34$, $P < 0.001$, $n = 363$) and till-slope ($r_s = -0.15$, $P < 0.001$, $n = 236$), whereas the organic layer thickness–bedrock slope correlation did not significantly differ from zero ($r_s = 0.03$, $P = 0.82$, $n = 54$; Table 2). A scatter plot of these relationships showed that deep organic layers (mean = 64 cm) were largely confined to clayey mineral soil, whereas shallower organic layers (mean = 25 cm) were typically located on till (Fig. 4). TWI was correlated with the presence of clay ($r_s = 0.13$, $P < 0.05$), till ($r_s = 0.26$, $P < 0.001$) and bedrock parent materials ($r_s = 0.38$, $P < 0.01$). Higher values of TWI (≥9) are mainly associated with areas having clayey mineral soils (Fig. 4). Stratification of the whole dataset by surficial deposits slightly reduced OLT variability within the clay, till and bedrock. Coefficients of variation are 0.42, 0.40, and 0.30, respectively, but stratification was less successful in improving correlation coefficients between individual topographic variables and organic layer thickness. In fact, OLT distribution at the landscape scale could obviously not be explained by simple bivariate relationships between OLT and individual predictor variables. In addition, the higher coefficient of variation for the whole OLT dataset (CV = 0.58) suggested a strong interaction between the different predictor variables and the spatial distribution of organic layer thickness. To reduce this variability in the whole dataset, a quantitative subdivision of the landscape into new datasets covering smaller and more homogeneous areas was undertaken.

### 3.2. Regression tree-based model evaluations

Results for the regression tree-based models that we developed using only mineral soil topographic variables (Model 1) and all the predictor variables (mineral soil topography and surficial deposits; Model 2) are illustrated in Table 3 and Figs. 5 and 7. Table 3 summarises the statistics obtained during model building and the regression tree criteria used in predicting OLT for regression tree-based models 1 and 2. Each of the 653 sampling locations were assigned to one of the resulting landscape units (A to F for model 1; A to J for model 2). In both models, the predictor variables that were used to generate the splits were mineral soil slope, surficial deposits, TWI and aspect. These four variables alone were important in predicting OLT over the landscape (Figs. 5, 7 and Table 3). Mineral soil curvature variables (mean curvature, plan curvature and profile curvature) were not found to contribute to the development of either regression tree-based model, suggesting that they did not play a role in controlling OLT at the landscape scale.

#### 3.2.1. Regression tree-based model 1

Model 1, based on topographic variables only, resulted in six landscape units and had a prediction quality of $R^2_{adj} = 0.34$, $r = 0.58$ and $RMSE = 23$ (Table 3). In model 1, the first node at which the entire dataset was initially subdivided into two groups, was based on slope ≤2% versus slope >2%. This resulted in areas of higher and lower organic layer thickness, respectively. Areas with slopes ≤2% were further subdivided at a second node into two landscape units (A and B, with mean organic layer depths of 43 cm and 68 cm, respectively), based on a TWI threshold value of 7 (Table 3). Within areas with slopes >3.5%, organic layers were deeper on north- and east-facing slopes (landscape unit D) compared to south- and west-facing areas (landscape units E and F) (Fig. 5, Table 3). Moderate OLT were found for areas with slopes >2% and ≤3.5% (Landscape unit C; mean OLT = 41 cm). These results supported our hypothesis that mineral soil topography has a significant influence on the spatial distribution of OLT. The predictive thematic map of landscape units (Fig. 6), indicated that 46.8% (33.6 ha) of the investigated area correspond to the high paludification category (landscape unit B), 43.4% (31.2 ha) to the moderate ones (landscape units A, C and D), and 9.8% (5.7 ha) to the non-paludified category (landscape units E and F) (Table 4). The confusion matrix between the measured paludification categories and the modelled ones showed a good overall accuracy of 74% of the sites (Table 4). The highly paludified category had the highest producer's accuracy (83%) followed by moderate and null categories with 74% and 57%, respectively (Table 4).

#### 3.2.2. Regression tree-based model 2

Model 2, based on all predictor variables, showed a substantial improvement in prediction quality ($R^2_{adj} = 0.52$, $r = 0.72$ and $RMSE = 19$; Table 3). The number of resulting landscape units was higher compared to model 1 and, consequently, some landscape units had few observations (i.e., Landscape units C and H in Table 3 and Fig. 7). The highest OLT was found on clayey surficial deposit with slopes between 2 and 3.7% (landscape units B and G with mean organic layer thicknesses of 71 cm and 53 cm, respectively), whereas shallow OLT (non-paludified) was associated with south- and west-facing areas

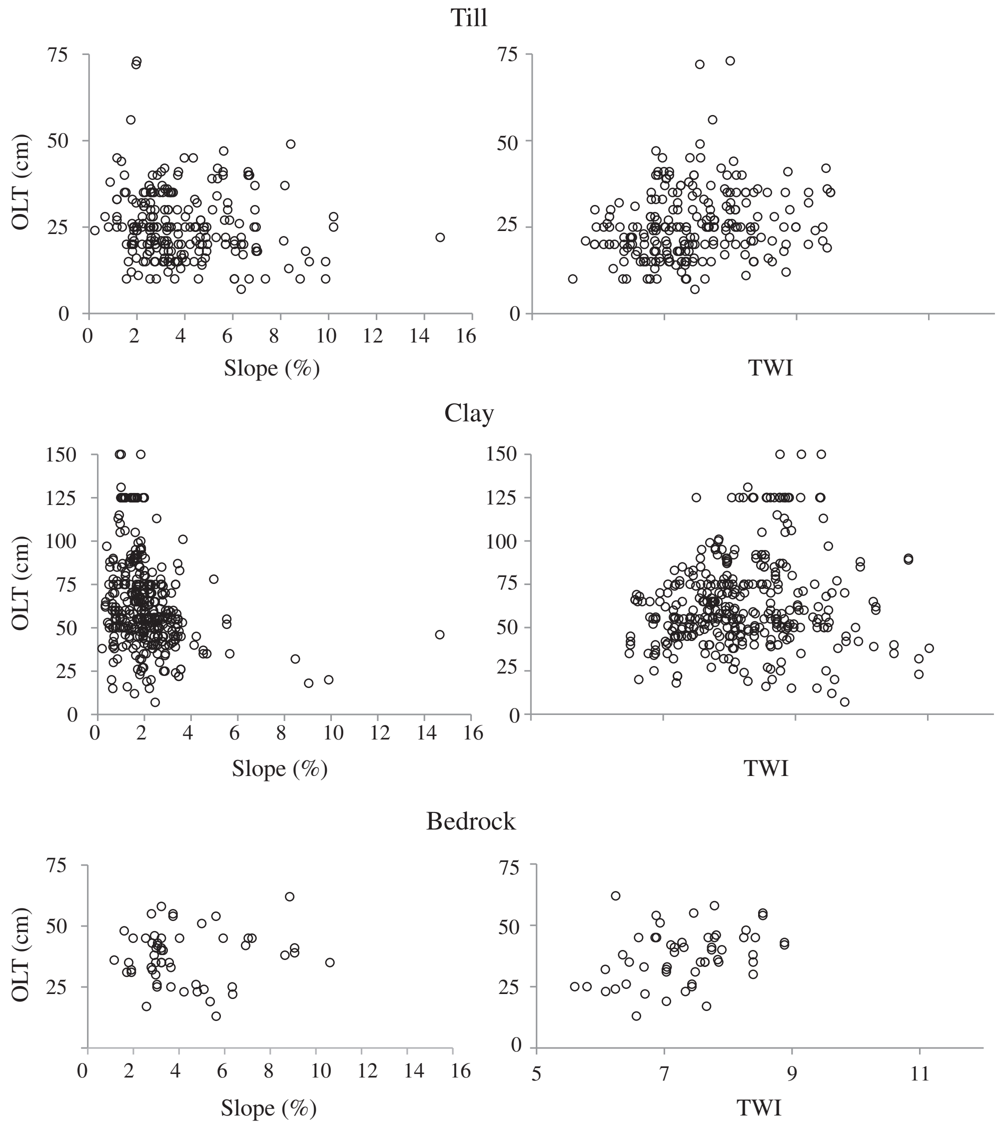


**Fig. 4.** Relationship between organic layer thickness and selected topographic variables for the three different surficial deposits (Till, Clay and Bedrock).

**Table 3**
Regression tree-based models that were used in this study to explain organic layer thickness and their statistics.

| Model | Terminal landscape unit splits | $n$ | Mean (cm) | $r$ | $R^2_{adj}$ | RMSE |
|---|---|---|---|---|---|---|
| Model 1 | | | | 0.58 | 0.34 | 23 |
| | A) Slope ≤ [2%]**, TWI ≤ [7]* | 32 | 43 | | | |
| | B) Slope ≤ [2%]**, TWI > [7]* | 234 | 68 | | | |
| | C) Slope > [2%]**, Slope ≤ [3.5%]** | 240 | 41 | | | |
| | D) Slope > [3.5%]**, Aspect [N&E]** | 46 | 41 | | | |
| | E) Slope > [3.5%]**, Aspect [S] † | 78 | 21 | | | |
| | F) Slope > [3.5%]**, Aspect [W] † | 23 | 25 | | | |
| Model 2 | | | | 0.72 | 0.52 | 19 |
| | A) Slope ≤ [2%]**, SurfDep [Till]** | 39 | 26 | | | |
| | B) Slope ≤ [2%]**, SurfDep [Clay]* | 220 | 71 | | | |
| | C) Slope ≤ [2%]**, SurfDep [Bedrock]* | 7 | 37 | | | |
| | D) Slope > [2%]**, SurfDep [Till]**, TWI ≤ [7]**, Aspect [N&E]** | 18 | 35 | | | |
| | E) Slope > [2%]**, SurfDep [Till]**, TWI ≤ [7]**, Aspect [S&W]** | 102 | 20 | | | |
| | F) Slope > [2%]**, SurfDep [Till]**, TWI > [7]** | 77 | 28 | | | |
| | G) Slope > [2%]**, SurfDep [Clay]**, Slope ≤ [3.7%]† | 130 | 53 | | | |
| | H) Slope > [2%]**, SurfDep [Clay]**, Slope > [3.7%]† | 13 | 39 | | | |
| | I) Slope > [2%]**, SurfDep [Bedrock]**, TWI ≤ [7] † | 27 | 34 | | | |
| | J) Slope > [2%]**, SurfDep [Bedrock]**, TWI > [7] † | 20 | 43 | | | |

**, * and † statistically significant at $P < 0.001$, $P < 0.01$ and $P < 0.05$, respectively. $r$ refers to correlation between measured and predicted values. Mean refers to mean organic layer thickness. RMSE = root mean square error. SurfDep refers to surficial deposit. N, E, S and W indicate north, east, south and west aspect directions, respectively.

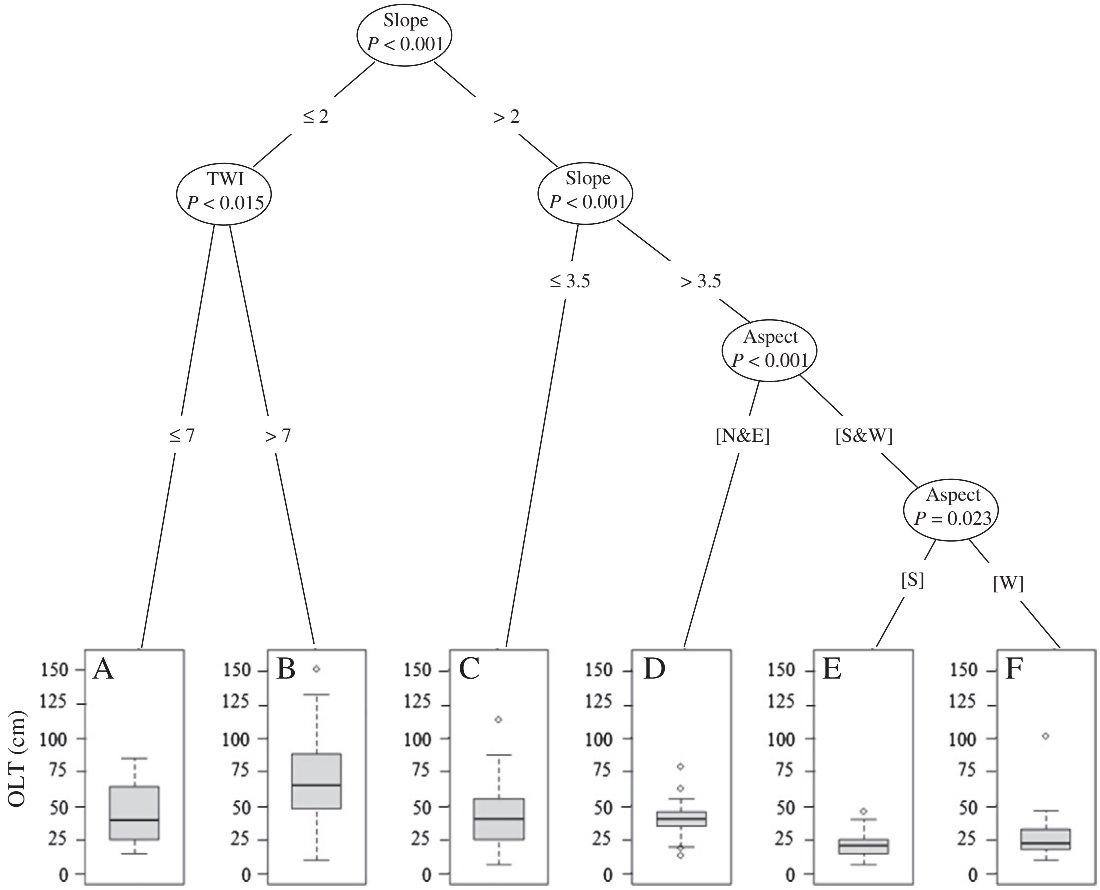


**Fig. 5.** Graphical representation of the regression tree model 1 in Table 3. The distribution of OLT in the resulting landscape units nodes (A to F) is visualised via box and whisker plots. The lower and upper edges of the box represent the 25th and 75th percentiles, and the median is represented by the bar in the middle of the box. The whiskers showed the largest and smallest values, and outliers are represented by individual points.

situated on till, with slopes >2% and TWI ≤ 7 (landscape unit E with mean OLT of 20 cm). Lower OLT was found on bedrock with slope ≤2% and slope >2% (Landscape units C and I with a mean OLT of 34 cm and 37 cm, respectively) and on till (Landscape units A, F and H with a mean OLT of 26 cm, 28 cm and 39 cm, respectively). Areas on bedrock with slope >2% were most effectively subdivided on the basis of the TWI into lower and moderate OLT landscape units (I and J, respectively) (Table 3 and Fig. 7). The moderate OLT unit was associated with a higher TWI (>7) suggesting that landscape unit J represents zones of soil water saturation.

## 4. Discussion

### 4.1. Individual relationship trends

The negative correlation between OLT and mineral soil slope indicated that the organic layer tended to be shallower in areas with high slopes and deeper in areas with low slopes. Similar results were found in other studies on ground surface slopes (i.e. Laamrani et al., 2013b; Simard et al., 2009).

Higher values of TWI are mainly associated with clayey mineral soil areas, which are the best candidates for high soil moisture content and water accumulation. These results are similar to those of other studies that found moisture-saturated sites were the most highly paludified areas (Fenton et al., 2005; Lavoie et al., 2005). When compared to a previous study that was conducted at the surface by Laamrani et al. (2013b), relationships between mineral soil aspect and OLT had similar trends. In contrast to the previous study, convex and concave mineral soil curvature variables (mean curvature, plan curvature and profile curvature) were found to be greater and more statistically significant compared to those computed at the ground surface, presumably because of depressional features that were revealed in the mineral soil topography.

### 4.2. Regression tree-based modelling approach

Mineral soil slope was involved in all landscape unit subdivisions in both models (1 and 2) and was the first level of splitting (Figs. 5 and 7), suggesting that OLT was largely controlled by the mineral soil slope at the landscape level. Alone, mineral soil slope explained 28% of the variation in the whole dataset (not shown). In addition to confirming the importance of mineral soil slope effects on OLT at the landscape scale, which had been previously reported for the surface layers within the Clay Belt (i.e., Giroux et al., 2001; Laamrani et al., 2013b; Simard et al., 2009), our study also quantified the threshold (2%) at which mineral soil slope could be used to discriminate units with deeper versus moderately shallow organic layers. Furthermore, for model 1, a slope threshold 3.5% seemed to represent a cutpoint for discriminating between paludified and non-paludified areas.

This study showed that higher OLT was found on north- and east-facing slopes (lower exposure to solar radiation). The higher OLT might be explained by the fact that north- and east-facing areas are colder and allow more *Sphagnum* moss to accumulate. This finding was similar to what was reported for the ground surface by Johnson et al. (2009). In contrast to our results, Laamrani et al. (2013b) found higher organic layer to accumulate on southwest-, west- and northwest facing slopes (see map of OLT, Figure 7 in Laamrani et al., 2013b).

Despite the significant correlations found between OLT and individual stratified curvature variables, the latter were not involved in any prediction of the OLT distribution through either regression model.

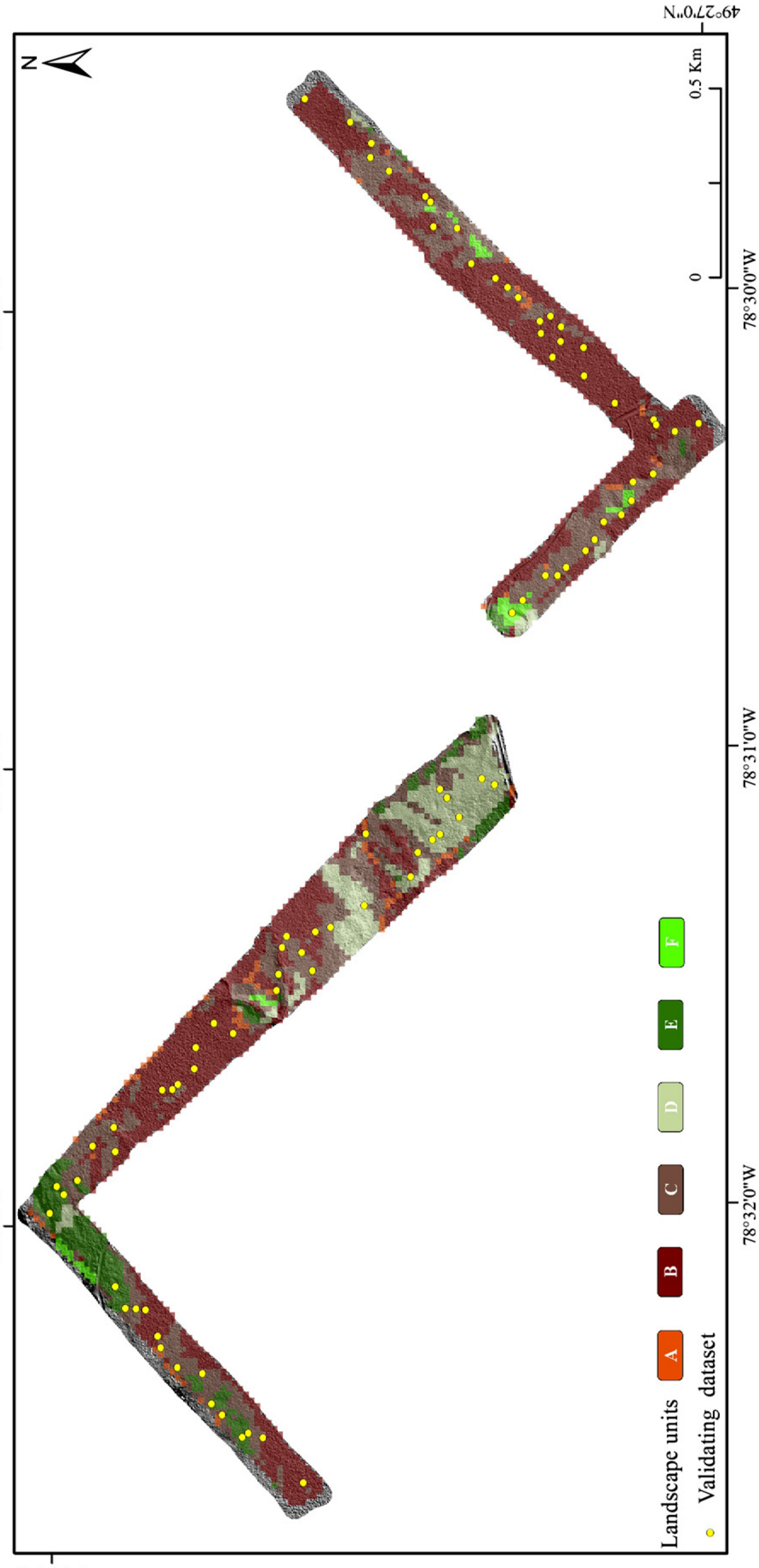


**Fig. 6.** Map showing the distribution of the landscape units in the study area based on regression tree model 1 in Table 3.

**Table 4**
Accuracy assessment and related statistics of map prediction of the landscape units, based on regression tree model 1.

| Landscape units | Area | | OLT (cm) | Paludification category | Area | | Producer accuracy | Overall accuracy |
|---|---|---|---|---|---|---|---|---|
| | % | ha | | | % | ha | | |
| B | 46.8 | 33.6 | 68 | High | 46.8 | 33.6 | 83% | 74% |
| A | 2.5 | 1.8 | 43 | Moderate | | | | |
| C | 29.5 | 21.2 | 41 | Moderate | 43.4 | 31.2 | 74% | |
| D | 11.4 | 8.2 | 41 | Moderate | | | | |
| E | 8.0 | 5.7 | 21 | Null | 9.8 | 7.0 | 57% | |
| F | 1.8 | 1.3 | 25 | Null | | | | |

OLT: organic layer thickness. Overall accuracy is computed by dividing the total correctly classified sites on the map by the total number of sites in the confusion matrix. Producer accuracy indicates the probability of a field measurement site being correctly classified on the map (measure of class accuracy).

One possible reason that could explain why curvature variables effect was masked is that the variation in the mineral soil curvature, at the local scale, was too small to be captured by the 15 m-resolution digital model.

Surficial deposits and TWI also contributed to the landscape unit partitioning for both regression tree models. Therefore, under conditions where slopes were ≤2%, clayey surficial deposit and TWI > 7, models 1 and 2 resulted in a homogeneous unit (B), representative of high paludification conditions. Landscape units B for both models seem to represent areas with conditions that may be less favourable for tree growth since the presence of thick organic layer combined with wet conditions on flat terrain is expected to limit tree establishment and productivity (Lavoie et al., 2007); this was supported by an on-going study that deals with the effect of organic layer thickness and slope on forest productivity (Laamrani et al.; unpublished results). They found that in average, landscape unit B showed the lowest stand volumes, estimated for trees with diameters at breast height (dbh) greater than nine cm, with 83 $m^3$/ha and 80 $m^3$/ha for models 1 and 2, respectively. In addition, evidence from field observations, together with Fig. 6 and aerial photos, indicated that landscape unit B most likely occur in both permanently and non-permanently paludified areas.

The TWI threshold of 7 was also used as splitting rule in model 2 to discriminate between low (landscape unit I) and moderately (landscape unit J) paludified bedrock with slopes >2%. Our field observations and Fig. 6 indicated that most of the sampling points in landscape unit J (higher TWI values) were located in topographic depressions at mid-slope (i.e., concave bedrock irregularities). This was consistent with other studies, which found that TWI describes the distribution and extent of soil moisture zones; the largest values were predicted in topographic hollows at higher elevation (Bou Kheir et al., 2010); and therefore, TWI could be used as a means of delineating and classifying landforms (Burrough et al., 2000; MacMillan et al., 2000). In addition, the lack of correlation between bedrock slope and OLT ($r_s = 0.03$, $P = 0.82$, Table 3) was presumably related to these bedrock irregularities. These topographic conditions favour high moisture resulting in organic layer accumulation, the development of a deeper organic layer (paludification) that is mainly composed of a thick Of horizon (Laamrani et al., 2013a; Lafleur et al., 2010; Lavoie et al., 2007), and are most likely specific to permanent paludification sites. We expected that these depressions would affect many of measured surface properties such as water movement in the near surface organic soil horizon, water infiltration, tree establishment and productivity.

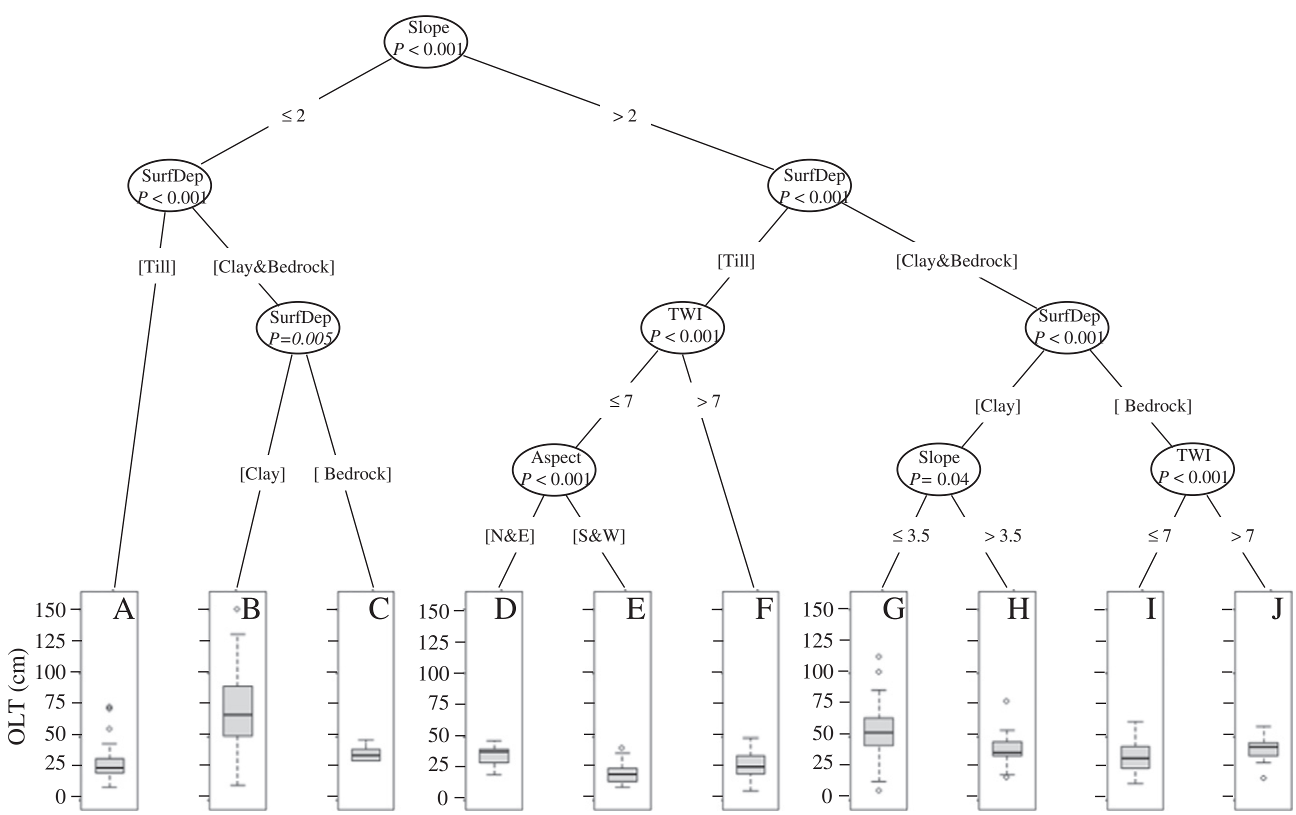


**Fig. 7.** Graphical representation of regression tree model 2 with the distribution of organic layer thickness in terminal nodes (A to J) visualised via box plots. Description of each component of the box and whiskers plot is given in Fig. 5.

Overall, the model that was based only on mineral soil topography explained 34% of the variation in the dataset. The model that was based on mineral soil topography, together with surficial deposits, had the greatest predictive power ($R^2_{adj} = 0.52$). For most spatial models, coefficients of determination ($R^2$) $\leq 0.5$ are common, whereas $R^2$ values that are greater than 0.7 are unusual (Dahlke et al., 2009). For both of our models, TWI made a significant contribution to estimating moderate to highly paludified landscapes, since it is a predictor of zones of saturation, and thick organic layers often accumulate in lowlands. Except for landscape unit J, which was assigned to the permanent paludification type in this study, both models were unable to further subdivide landscape units (i.e., landscape unit B) into reversible and permanent types. This suggested that both factors (time and topography) interact together. Both models (i) produced simpler models that were easier to understand, (ii) represented landscape units that were meaningful in terms of the physical processes of OLT variability and distribution, and (iii) consisted of a small number of rules. Model 1 could be easily and quickly implemented for making predictions whenever a DEM is available with OLT measurements (Fig. 6), but model 2 can only be used in situations where spatial information on surficial deposits (clay, till, bedrock) exist, which is not the case in most of the Forest inventory maps.

### 4.3. Management implications

The results of this study are important for landscape management for several reasons:

(1) Understanding how surface topography is related to OLT is an important first step in predicting and mapping forest productivity across landscapes. This information will aid the forest managers in predicting potential saturation zones, where an organic layer often accumulates and will help them to adopt the appropriate forest management practices (i.e., field preparation treatments and replanting). For example, TWI is simple in concept, easily defined, and provides an intuitive notion of wetness. Consequently, it can be used to better manage forest resources where high soil moisture limits productivity.

(2) In order to maintain or improve forest productivity in the Clay Belt region, management strategies should focus on sloping sites (i.e., >2.3%) rather than on almost flat sites (≤2%) that are associated with deep organic layer. The latter are often not suitable for tree plantations (Lafleur et al., 2010), provide few ecological or economic motives to manage soils with low slopes (Simard et al., 2009), and are expected to limit the use of equipment that would be required for mechanical site preparation and harvesting within the highly paludified areas (Lavoie et al., 2007).

(3) This study is part of a larger project that deals with the effects of environmental variables and forest harvesting on paludification and was conducted prior to implementation of recent forest management prescriptions (harvesting, site preparation, and planting). Therefore, the results and data from this study could be used to determine the long-term impact of forest management practices (i.e., forest harvesting, field preparation treatments, and replanting) on the original organic layer properties.

(4) Results from this study have demonstrated that mineral soil topography has a significant influence on the spatial distribution of OLT and that these relationships can be used for partitioning the landscape and, therefore, can help in future planning of landscape management. For instance, they can be used for defining (i) promising areas where efforts and investments should be made to obtain higher productivity after logging and planting and (ii) vulnerable areas where structure and biodiversity of paludified forest can be preserved.

## 5. Conclusions

To our knowledge, this study was the first to link topographic variables that were extracted at the surface of the mineral soil to different degrees (representing organic layer thickness) and types of paludification at the landscape-scale. The analysis of topography at the mineral soil surface within the Clay Belt region demonstrated correlations between individual topographic variables (slope, aspect, TWI), surficial deposits and organic layer thickness. These correlations were found to be relatively weak, and indicated that, at the landscape scale, OLT and its distribution cannot be adequately explained by simple bivariate relationships. Consequently, two regression tree-based models (models 1 and 2) were developed in this study and provided insight into set of predictor variables that are most important for OLT distribution. Mineral soil slope, TWI and aspect proved to be highly correlated with OLT for both models. Model 1 based on mineral soil surface topography explained 34% of the variation in organic layer thickness, whereas model 2 based on mineral soil surface topography and surficial deposits explained 52%.

Regression tree Model 1 allowed the combination of different maps (slope, TWI and aspect) for producing a landscape unit map, upon which OLT was determined and related to increasing paludification categories. A good overall accuracy of 74% was achieved for the resulting model 1 map. One of the most important finding that was revealed by model 2 indicated that bedrock irregularities (i.e., depressions) modified topographic control of wetness and promoted the advancement of permanent paludification. Except for landscape unit J, which was assigned to the permanent paludification type, both models were unable to further subdivide the resulting landscape units (i.e., landscape unit B) into reversible and permanent types. Future work will focus on the use of additional topographic variables (i.e., topographic slope position) and other remote sensing techniques (i.e., automated classification) to discriminate between the two categories of paludification (reversible and permanent) within a larger LiDAR covered area (100 $km^2$).

## Acknowledgements

Funding for this research was provided by the Natural Sciences and Engineering Research Council of Canada (NSERC), Fonds Québécois de la Recherche sur la Nature et les Technologies (FQRNT), Université du Québec en Abitibi-Témiscamingue (UQAT) and Université du Québec à Montréal (UQAM), the Regional Conference of Elected representatives of James Bay (CREBJ), NSERC-UQAT-UQAM Chair in Sustainable Forest Management, Centre d'Étude de la Forêt — Centre for Forest Research (CEF-CFR) and Tembec Inc. We are grateful to Dr. Benoît St-Onge (UQAM) for his assistance with the processing of raw LiDAR data, Dr. Jean Veillette (Geological Survey of Canada) for his assistance with surficial deposits characterisation, and Dr. W.F.J. Parsons (CEF-CFR) who revised the English and helped improve the quality of the manuscript. We also thank the editor and two anonymous reviewers for their helpful comments throughout the review process.

## References

Blyth, E.M., Finch, J., Robinson, M., Rosier, P., 2004. Can soil moisture be mapped onto the terrain? Hydrol. Earth Syst. Sci. 8, 923–930.
Bou Kheir, R., Bøcher, P.K., Greve, M.B., Greve, M.H., 2010. The application of GIS based decision-tree models for generating the spatial distribution of hydromorphic organic landscapes in relation to digital terrain data. Hydrol. Earth Syst. Sci. 14, 847–857.
Burrough, P.A., Van Gaans, P.F.M., MacMillan, R.A., 2000. High-resolution landform classification using fuzzy k-means. Fuzzy Sets Syst. 113, 37–52.
Congalton, R.G., 1991. A review of assessing the accuracy of classifications of remotely sensed data. Remote Sens. Environ. 37, 35–46.
Crawford, R.M.M., Jeffree, C.E., Rees, W.G., 2003. Paludification and forest retreat in northern oceanic environments. Ann. Bot. 91, 213–226.
Dahlke, H.E., Behrens, T., Seibert, J., Andersson, L., 2009. Test of statistical means for the extrapolation of soil depth point information using overlays of spatial environmental data and bootstrapping techniques. Hydrol. Process. 23, 3017–3029.

Emili, L.A., Price, J.S., Fitzgerald, D.F., 2006. Hydrogeological influences on forest community type along forest–peatland complexes in coastal British Columbia. Can. J. For. Res. 36, 2024–2037.

Environment Canada, 2013. Canadian Climate Normals 1971–2000. Matagami weather station (Available online at http://www.ec.gc.ca/. Last accessed June 2013).

ESRI, 2011. ArcGIS Desktop: Release 10. Environmental Systems Research Institute, Redlands, CA, USA (Available online at http://help.arcgis.com/en/arcgisdesktop/10.0/help/; last accessed April 2013).

Everitt, S., Hothorn, T., 2009. A Handbook of Statistical Analyses Using R, 2nd ed. CRC Press, Francis & Taylor Group.

Fenton, N., Lecomte, N., Légaré, S., Bergeron, Y., 2005. Paludification in black spruce (*Picea mariana*) forests of eastern Canada: potential factors and management implications. For. Ecol. Manag. 213, 151–159.

Fenton, N.J., Bergeron, Y., 2006. Facilitative succession in a boreal bryophyte community driven by changes in available moisture and light. J. Veg. Sci. 17, 65–76.

Fenton, N.J., Bergeron, Y., 2007. *Sphagnum* community change after partial harvest in black spruce boreal forests. For. Ecol. Manag. 242, 24–33.

Fenton, N.J., Simard, M., Bergeron, Y., 2009. Emulating natural disturbances: the role of silviculture in creating even-aged and complex structures in the black spruce boreal forest of eastern North America. J. For. Res. 14, 258–267.

Gessler, P.E., Moore, I.D., McKenzie, N.J., Ryan, P.J., 1995. Soil-landscape modelling and spatial prediction of soil attributes. Int. J. Geogr. Inf. Sci. 9, 421–432.

Giroux, J.F., Bergeron, Y., Veillette, J.J., 2001. Dynamics and morphology of giant circular patterns of low tree density in black spruce stands in northern Quebec. Can. J. Bot. 79, 420–428.

Greve, M.H., Kheir, R.B., Greve, M.B., Bøcher, P.K., 2012a. Quantifying the ability of environmental parameters to predict soil texture fractions using regression-tree model with GIS and LIDAR data: the case study of Denmark. Ecol. Indic. 18, 1–10.

Greve, M.H., Kheir, R.B., Greve, M.B., Bøcher, P.K., 2012b. Using digital elevation models as an environmental predictor for soil clay contents. Soil Sci. Soc. Am. J. 76, 2116–2127.

Güntner, A., Seibert, J., Uhlenbrook, S., 2004. Modeling spatial patterns of saturated areas: an evaluation of different terrain indices. Water Resour. Res. 40, W051141–W0511419.

Hothorn, T., Hornik, K., Zeileis, A., 2006. Unbiased recursive partitioning: a conditional inference framework. J. Comput. Graph. Stat. 15, 651–674.

Johnson, K.D., Scatena, F.N., Johnson, A.H., Pan, Y., 2009. Controls on soil organic matter content within a northern hardwood forest. Geoderma 148, 346–356.

Laamrani, A., Valeria, O., Cheng, L.-Z., Bergeron, Y., Camerlynck, C., 2013a. The use of Ground Penetrating Radar for remote sensing the organic layer-mineral soil interface in paludified boreal forests. Can. J. Remote. Sens. 39, 1–15.

Laamrani, A., Valeria, O., Fenton, N., Bergeron, Y., 2013b. Landscape-scale influence of topography on organic layer accumulation in paludified boreal forests. For. Sci. http://dx.doi.org/10.5849/forsci.13-025 (Article first published online: 19 September 2013).

Lafleur, B., Fenton, N.J., Paré, D., Simard, M., Bergeron, Y., 2010. Contrasting effects of season and method of harvest on soil properties and the growth of black spruce regeneration in the boreal forested Peatlands of Eastern Canada. Silva Fenn. 44, 799–813.

Lavoie, M., Pare, D., Fenton, N., Groot, A., Taylor, K., 2005. Paludification and management of forested peatlands in Canada: a literature review. Environ. Rev. 13, 21–50.

Lavoie, M., Harper, K., Paré, D., Bergeron, Y., 2007. Spatial pattern in the organic layer and tree growth: a case study from regenerating *Picea mariana* stands prone to paludification. J. Veg. Sci. 18, 213–222.

MacMillan, R., Pettapiece, W., Nolan, S., Goddard, T., 2000. A generic procedure for automatically segmenting landforms into landform elements using DEMs, heuristic rules and fuzzy logic. Fuzzy Sets Syst. 113, 81–109.

Moore, I.D., Lewis, A., Gallant, J.C., 1993. Terrain attributes: estimation methods and scale effects. In: Jakeman, A.J., Beck, M.B., McAleer, M.J. (Eds.), Modelling Change in Environmental Systems. Wiley, London, pp. 189–214.

Peucker, T.K., Fowler, R.J., Little, J.J., Mark, D.M., 1978. The triangulated irregular network. Proceedings, Digital Terrain Models (DTM) Symposium, American Society of Photogrammetry, May 9–11, 1978, St. Louis, Missouri, pp. 516–540.

R Development Core Team, 2011. R: A Language and Environment for Statistical Computing. R Foundation for Statistical Computing, Vienna, Austria (URL http://www.R-project.org/).

Rothwell, J.J., Futter, M.N., Dise, N.B., 2008. A classification and regression tree model of controls on dissolved inorganic nitrogen leaching from European forests. Environ. Pollut. 156, 544–552.

Seibert, J., Stendahl, J., Sorensen, R., 2007. Topographical influences on soil properties in boreal forests. Geoderma 141, 139–148.

Simard, M., Lecomte, N., Bergeron, Y., Bernier, P.Y., Pare, D., 2007. Forest productivity decline caused by successional paludification of boreal soils. Ecol. Appl. 17, 1619–1637.

Simard, M., Bernier, P.Y., Bergeron, Y., Paré, D., Guérine, L., 2009. Paludification dynamics in the boreal forest of the James Bay Lowlands: effect of time since fire and topography. Can. J. For. Res. 39, 546–552.

Sørensen, R., Zinko, U., Seibert, J., 2006. On the calculation of the topographic wetness index: evaluation of different methods based on field observations. Hydrol. Earth Syst. Sci. 10, 101–112.

Southee, F.M., Treitz, P.M., Scott, N.A., 2012. Application of lidar terrain surfaces for soil moisture modeling. Photogramm. Eng. Remote Sens. 78, 1241–1251.

Veillette, J.J., 1994. Evolution and paleohydrology of glacial Lakes Barlow and Ojibway. Quat. Sci. Rev. 13, 945–971.

Veillette, J.J., Paradis, S.J., Buckle, J., 2005. Bedrock and surficial geology of the general area around Rouyn-Noranda, Quebec and Ontario. In Metals in the environment around smelters: the GSC-MITE point sources project, Rouyn-Noranda (Quebec) and Belledune (New Brunswick). Bull. Geol. Surv. Can. 584, 1–16.

Vepakomma, U., St-Onge, B., Kneeshaw, D., 2011. Response of a boreal forest to canopy opening: assessing vertical and lateral tree growth with multi-temporal lidar data. Ecol. Appl. 21, 99–121.

Vygodskaya, N.N., Groisman, P.Y., Tchebakova, N.M., Kurbatova, J.A., Panfyorov, O., Parfenova, E.I., Sogachev, A.F., 2007. Ecosystems and climate interactions in the boreal zone of northern Eurasia. Environ. Res. Lett. 2, 1–7.

Webster, K.L., Creed, I.F., Beall, F.D., Bourbonnière, R.A., 2011. A topographic template for estimating soil carbon pools in forested catchments. Geoderma 160, 457–467.

Work, T.T., St-Onge, B., Jacobs, J.M., 2011. Response of female beetles to LIDAR derived topographic variables in Eastern boreal mixedwood forests (Coleoptera, Carabidae). ZooKeys 147, 623–639.

Zinko, U., Seibert, J., Dynesius, M., Nilsson, C., 2005. Plant species numbers predicted by a topography-based groundwater flow index. Ecosystems 8, 430–441.